

AJTE99-6302

PROGRESS IN DIRECT NUMERICAL SIMULATION OF TURBULENT HEAT TRANSFER

NOBUHIDE KASAGI

Department of Mechanical Engineering
The University of Tokyo
Hongo 7-3-1, Bunkyo-ku
Tokyo 113-8656, Japan
E-mail: kasagi@thtlab.t.u-tokyo.ac.jp

OAKI IIDA

Department of Mechanical Engineering
Nagoya Institute of Technology
Gokiso-cho, Showa-ku
Nagoya 466-8555, Japan
E-mail: iida@heat.mech.nitech.ac.jp

Keywords: *Turbulent Heat Transfer, Direct Numerical Simulation, Prandtl Number, Buoyancy, Control*

ABSTRACT

With high performance computers, reliable numerical methods and efficient post-processing environment, direct numerical simulation (DNS) offers valuable numerical experiments for turbulent heat transfer research. In particular, one can extensively study the turbulence dynamics and transport mechanism by visualizing any physical variable in space and time. It is also possible to establish detailed database of various turbulence statistics of turbulent transport phenomena, while systematically changing important flow and scalar field parameters. The present paper illustrates these novelties of DNS by introducing several examples in recent studies. Future directions of DNS for turbulence and heat transfer research are also discussed.

In the following, with introductory remarks on computational requirement for respectable DNS, progress in numerical techniques is first reviewed. Then, an effort to reveal the effect of Prandtl number on turbulent heat transfer is sketched with an emphasis on the new techniques developed for making DNS over a wide range of Prandtl number possible. Both methods of saving grid points and Lagrangian particle tracking are found very useful in the future work on turbulent heat and mass transfer.

The complex buoyancy effects on turbulent transport are discussed in a series of DNSs of horizontal and vertical channel flows. It is found that the buoyancy effect appears much differently depending upon the directional alignment of the

buoyant force and the mean flow. In the vertical flow, the buoyancy effect results in an increased or decreased Reynolds number effect, which appears through a change in the Reynolds stress distribution and hence in the shear production rate of turbulent kinetic energy near the wall. In the horizontal flow, however, it causes substantial alternation in the turbulence structures and transport mechanism so that the resultant heat transfer coefficient would behave in a much more complex manner. The thermal plumes and internal gravity waves characteristic of these flows play an important role in the interaction with the quasi-coherent structures of wall turbulence.

DNSs of the channel flow under active turbulence and heat transfer control are discussed finally. In these simulations, an array of micro deformation actuators on a wall surface or intelligent micro particles are tested as control schemes. It is shown that these sophisticated devices possibly bring about notable friction drag reduction and heat transfer enhancement. A perspective view is given that DNS will be even more useful in evaluating future turbulence control methodologies based on new algorithms such as optimum control theory and neural networks. These simulations have been triggered by the rapid development of microelectromechanical systems (MEMS) technology, but hopefully future DNSs will lead further development of MEMS-based controller units integrating micro sensors, micro actuators and IC.

INTRODUCTION

Turbulent momentum and scalar transport plays a key role in many engineering applications and will be of growing importance in global environmental problems. For instance, it is necessary to predict flow and heat transfer characteristics under design conditions, if one has to establish efficient and safe industrial systems such as aircrafts, ships, automobiles and power plants. Control of thermo-fluids phenomena in various equipment and production processes is crucial to keeping high quality, reliability and safe operation of products. Hence, much effort has been devoted to developing methodologies for prediction and control of various turbulent flows and associated transport phenomena.

In the early 1980's, with the advancement of large scale computers, direct numerical simulation (DNS, hereafter) of turbulent flow and heat transfer became possible. Later, the use of DNS rapidly spread in the turbulence research community. DNSs are three-dimensional, time-dependent numerical solutions of the Navier-Stokes and scalar transport equations that govern the evolution of flow and scalar fields. These governing equations do not involve any turbulence models. Hence, a DNS must be executed on a fine grid system to capture all scales arising in turbulent processes. Despite this demanding nature, DNS has proved to be a valuable tool for the fundamental research of turbulent transport phenomena (Reynolds, 1990; Kasagi & Shikazono, 1995; Moin & Mahesh, 1998; Kasagi, 1998).

In this paper, numerical methods for DNS are first reviewed briefly and then the recent progress in the applications of DNS is illustrated by introducing typical examples. Namely, DNSs of turbulent heat transfer in a plane channel at various Prandtl numbers are sketched. Then, the complex effects of buoyancy on turbulence and heat transfer are explored with a series of DNSs. Finally, trial computations for possible active turbulence control are presented. The authors' view on future development is given, when appropriate.

NUMERICAL METHODS OF DIRECT NUMERICAL SIMULATION

Because a turbulent flow phenomenon contains a broad range of dynamically significant scales, its DNS must be executed in a computational domain large enough to contain the largest eddies, while keeping the grid spacing fine enough to resolve the smallest eddies. The ratio of the largest to smallest length scales in a turbulent flow is roughly estimated to be proportional to the $3/4$ power of the flow Reynolds number Re in each direction, so that the total number of grid points N required in a DNS is proportional to $Re^{9/4}$. The time increment in advancing the numerical integration must be as small as the smallest eddy's turnover time (and a Courant number also be

sufficiently small), whilst the total length of integration should be much larger than the largest eddy's turnover time in order to obtain well converged turbulence statistics. The ratio of these largest to smallest time scales is roughly proportional to $Re^{1/2}$. Thus, as the Reynolds number increases, the numbers of grid points and time steps inevitably increase rapidly.

The above requirement of DNS is even more serious, once additional scales, which are out of the range of turbulence scales, are introduced or imposed. For example, thermal turbulence microscales should also be captured when turbulent heat transfer is to be simulated (Kim & Moin, 1989; Kasagi & Shikazono, 1995), but this becomes difficult when the Prandtl number is very large. The essentially same problem arises in flows with mass transfer and chemical reactions. In a flow along a wall surface with artificial micro-groves (riblets), a large computational volume is hard to retain, because more grid points are required in order to represent the riblet shape with a sharp ridge (Choi et al., 1993a). In the simulations of multiphase flows, characteristic scales of interfacial dynamics (or waves) and of distributed particles and bubbles do not always stay within the range of turbulence scales, yet have remarkable interactions with turbulence. In flows under arbitrarily imposed unsteadiness, associated time scales must also be captured. These facts should be a major difficulty in DNSs of complex turbulent flows.

Continuous efforts have been directed toward improvement of the numerical methods of DNS. Spatial discretization schemes for DNS are categorized into spectral (Canuto et al., 1987), spectral element (Patera, 1984) and finite difference (Peyret & Taylor, 1983) methods. Among them, the spectral method should be most suitable to DNS because of its exponential convergence. It needs, however, linearization of governing equations with explicit or semi-implicit time advancement schemes. The channel flow simulation of Kim et al. (1987) is based on a pseudo-spectral method, which employs Fourier series in the two periodic directions and Chebyshev polynomial expansion in the wall-normal direction. The spectral method can be applied to geometrically complex flows by using mapping (coordinate transformation) or patching (Orszag, 1980). The former is used in the adaptive spectral method, which has been successfully employed in the DNSs of turbulent boundary layers (Spalart & Leonard, 1987), square duct flows (Madabhushi et al., 1993), turbulent flows over bumps (Carlson & Lumley, 1996) and gas-liquid interfacial turbulence (Lombardi et al., 1996).

The spectral element technique can be interpreted as a high-order finite element method (Peyret & Taylor, 1983). It has been applied to a DNS of turbulent flow over riblets (Chu & Karniadakis, 1993). Since it has both flexibility of finite element method and high accuracy of spectral method, it will

be more widely used in the future DNSs of engineering interest (Karniadakis & Henderson, 1998).

High-order finite difference schemes (Rai & Moin, 1991; Rai & Moin, 1993) and a compact finite difference scheme (Adam, 1977; Hirsh, 1977; Lele, 1992) have been extensively used and tested. The former was employed in the DNS of turbulent boundary layers by Rai & Moin (1993). In addition, the second-order finite difference scheme has been employed with a fractional step method in various flows, e.g., turbulent flows in a square duct (Gavrilakis, 1992), over riblets (Choi et al., 1993a), in a curved square duct (Zang et al., 1994) and along an oscillatory deforming wall (Mito & Kasagi, 1998).

Temporal discretization schemes adopted so far are an explicit scheme, a semi-implicit scheme (a combination of implicit and explicit schemes), and a fractional step method (Chorin, 1969; Temam, 1984). The semi-implicit scheme, with Adams-Bashforth method used for the nonlinear terms and Crank-Nicolson method for the linear terms, is often adopted (Kim et al., 1987), whilst the third-order Runge-Kutta method (Spalart et al., 1991) has also become popular. A fractional step method developed by Chorin (1969) and Temam (1984) is employed in many DNSs. With this scheme, solutions for velocity and pressure fields can be separated, and this leads to appreciable reduction in computational load. Kim & Moin (1985) uses a semi-implicit type fractional step method, with Adams-Bashforth method for the nonlinear terms and Crank-Nicolson method for the linear terms. This method has been modified to a high-order version by Rai & Moin (1991) and Le & Moin (1991), i.e., with a low-storage third-order Runge-Kutta method and a Crank-Nicolson method.

It is noted that recent DNS applications are also found in the research on multiphase turbulent flows. Gas-liquid interfaces, bubbles and particles are taken into account by sophisticated numerical techniques, e.g., level set (Sussman et al., 1994), CIP (Yabe & Aoki, 1991) and force (Fogelson & Peskin, 1988) methods. In particle-laden flows, interactions take place between fluid and particles, which should be properly taken into account (McLaughlin, 1994). When the particle concentration is dilute, only the force experienced by particles is calculated; this treatment is called one-way coupling (Pedinotti et al., 1992). Care must be taken of the degree of approximation in the equation of particle motion and also of the interpolation technique for the velocity field calculated by DNS. Current effort is being made to calculate also particles' forces acting on fluid (two-way coupling) for higher particle concentrations and in more general cases particle collisions, although only a few results have been reported (see, e.g., Elghobashi & Truesdell, 1993; Pan & Banerjee, 1996; Yamamoto et al., 1998).

APPLICATIONS OF DIRECT NUMERICAL SIMULATION

Novelty of DNS

A DNS can be regarded as a numerical experiment which replaces a laboratory experiment. Although the Reynolds number remains small to moderate, there are many attractive features in DNS, and some of them are to be worth mentioning below (Kasagi & Shikazono, 1995):

- (1) Unlike experimental measurement, DNS allows one to probe all the instantaneous flow variables such as velocities, pressures, and temperatures in space. Hence, turbulent structures and transport mechanisms can be analyzed in details through various theoretical and visualization techniques (Robinson, 1991; Kasagi et al., 1995).
- (2) Even experimental measurement techniques can be validated in simulated turbulent flow and thermal fields (Moin & Spalart, 1989; Suzuki & Kasagi, 1992).
- (3) DNSs provide precise turbulence statistics including pressure and any spatial derivatives, which are extremely difficult to measure. They are undoubtedly helpful for evaluating and developing turbulence models. The statistics and their budgets in various types of flows are available in tabulated forms at ftp sites (e.g., <http://www.thtlab.t.u-tokyo.ac.jp>).
- (4) The effects of various influential parameters can be studied systematically by DNS. Namely, dimensionless parameters such as Reynolds, Prandtl, Richardson, Rossby, and Hartmann numbers, can be systematically changed in DNSs. Wall injection/suction effects on turbulent heat transfer have been examined by Sumitani & Kasagi (1995).
- (5) Lastly, DNS can offer a chance to study even a virtual flow and heat transfer. This is particularly meaningful in evaluating possible turbulence control methodologies (Jung et al., 1992; Choi et al., 1994; Satake & Kasagi, 1996).

DNS of Turbulent Heat Transfer at Various Prandtl Numbers

If we extensively exploit DNS of turbulent heat transfer, the numerical as well as physical accuracy of DNS should be first confirmed. In particular, the velocity field should have been well examined before any argument in the heat transfer aspect is put forward. The DNS results have been repeatedly compared to the experimental data over the last decade. The most comprehensive verification has been made in the fully developed channel flow. In general, various statistical quantities and the turbulent structures visualized in the simulation are in close agreement with the experimental data and observation both qualitatively and quantitatively.

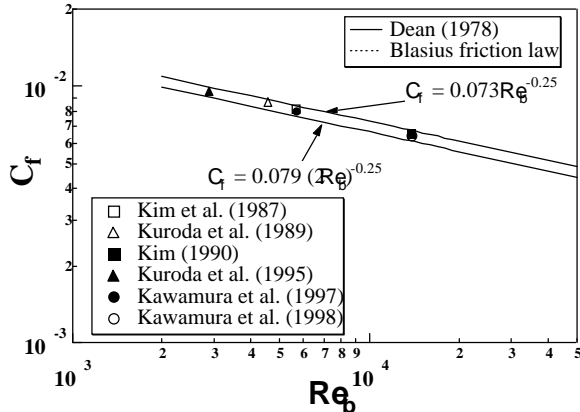


Figure 1 Friction coefficient

As a typical example, the friction coefficients reported by several workers are compared with empirical formula in Fig. 1. Four early simulations were made by using a pseudo-spectral method with Fourier series in the streamwise and spanwise directions and a Chebyshev polynomial expansion in the wall-normal direction, whilst two recent simulations were made by a second-order central finite difference method. Although the DNSs of Kim et al. (1987) and of Kuroda et al. (1989, 95) at the bulk Reynolds number of $Re_b = 2u_b\delta/\nu < 6000$ use sufficiently large computational volumes ($4\sim 5\pi\delta \times 2\delta \times 2\pi\delta$), the two of Kim (1990) and Kawamura et al. (1998) adopt a smaller volume ($2\pi\delta \times 2\delta \times \pi\delta$) at $Re_b \sim 14,000$ for saving computer storage. Here, δ is the channel half width. In these simulations, the spatial and temporal resolutions are sufficiently or marginally fine to capture all dynamically significant scales of turbulence. In spite of the difference in computational conditions, the calculated friction coefficients agree well with the formula of Dean (1978). Strictly speaking, all numerical results are smaller by a small fraction than the empirical formula, and this is because the aspect ratio of the channel is mostly about 10 in the experiments, but assumed to be

infinitely large in the DNSs.

Another example is shown in Fig. 2, where three root-mean-square velocity fluctuations divided by a local mean velocity are compared between the DNS of Kim et al. (1987) and experimental data of Kreplin & Eckelmann (1979) and Nishino & Kasagi (1989). Although the comparison in this figure is critical since both numerator and denominator have uncertainties, almost complete collapse is observed between the DNS and the data of Nishino & Kasagi, who used a three-dimensional particle tracking velocimeter. There are discernible errors in the near-wall data of Kreplin & Eckelmann's hot-film measurement. The reason for this has been found by Suzuki & Kasagi (1992) through their virtual calibration of hot-wires in a DNS data that those errors are inherent in finite dimensions of hot-wires, which can not assumed to be ideally small compared with the scales of turbulence diminishing toward the wall. Comparison has also been extended from mean velocity to up to the fourth-order moments of velocity fluctuations, and excellent agreement has been confirmed. Thus, it can be said that, as long as respectable computational schemes and numerical conditions are employed, DNS offers reliable statistical quantities of turbulence (also see, Kasagi & Shikazono, 1995).

Owing to a grid requirement, high Reynolds number DNS is a difficult task, but DNS of turbulent heat and mass transfer becomes even more difficult as the Prandtl (or Schmidt) number is increased. The ratio of the largest to smallest length scales in thermal turbulence is roughly proportional to $Re^{3/4} Pr^{1/2}$ at high Prandtl numbers (Batchelor, 1959; Tennekes & Lumley, 1972) and this means that the ratio of the grid points required for thermal field N_θ to that for velocity field N is proportional to $Pr^{3/2}$. For instance, N_θ/N is about 30 and 10^3 for $Pr = 10$ and 100, respectively. Thus, the DNS of turbulent heat transfer becomes much harder as Pr is increased. It is also noted that, when Pr is decreased, less grid resolution would be required, but a care must be taken so that the computational volume should be enlarged to capture larger scales of thermal turbulence.

Since the DNSs of turbulent heat transfer in channel flow at $Pr \sim 1$ were made at $Re_\tau = 180$ by Kim & Moin (1989), and at $Re_\tau = 150$ by Lyon & Hanratty (1991) and Kasagi et al. (1992), those at lower Pr were also carried out at $Re_\tau = 150$ by Kasagi & Ohtsubo (1993) and later at $Re_\tau = 180$ by Kawamura et al. (1997). Here, $Re_\tau (= u_\tau\delta/\nu)$ is the Reynolds number based on the friction velocity and the channel half width. The statistical quantities of thermal turbulence have been collected and even the budget terms in the transport equations of temperature variance, its dissipation rate and turbulent heat fluxes have been quantitatively evaluated. In particular, Kasagi & Ohtsubo (1993) claim that a major sink term for the turbulent heat flux

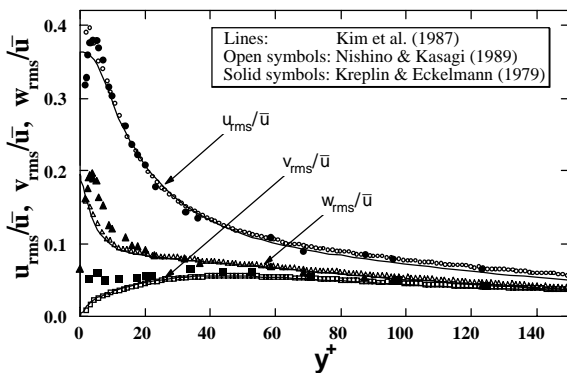


Figure 2 Root-mean-square turbulent velocity fluctuations divided by local mean velocity

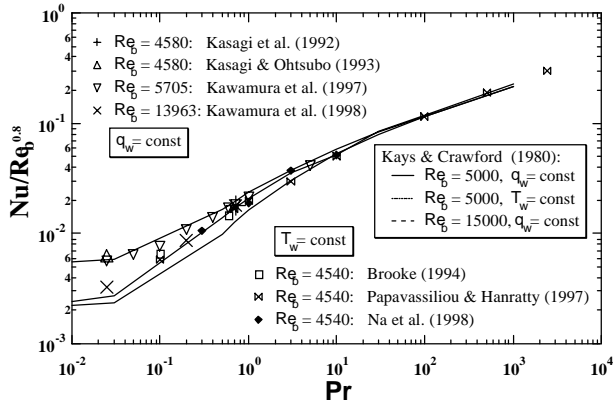


Figure 3 Dependence of heat transfer coefficient on Prandtl number

at low Pr numbers is a molecular dissipation, but not the pressure temperature-gradient correlation, which mainly breaks down the heat flux at higher Pr numbers. Furthermore, they have found that even for low Pr the major transport mechanisms are closely related with the quasi-coherent vortical structures of wall turbulence (Kasagi et al., 1995).

High Pr heat transfer is a classical, but challenging problem, of which DNS several recent workers have attempted. With a large scale parallel computer system, Kawamura et al. (1997) extended their DNS of turbulent heat transfer in a uniformly heated channel to $Pr = 5$ at $Re_\tau = 180$; this DNS is the first that has been run at sufficiently high Re and Pr numbers. The number of grids used for a computational volume of $6.4\delta \times 2\delta \times 3.2\delta$ is $256 \times 128 \times 256$, which is twice as many as that sufficient for the velocity field. The resultant grid spacing is 4.5 and 2.25 wall units in the streamwise and spanwise directions, respectively, while non-uniform spacing from 0.44 to 13.0 wall units is used in the wall-normal direction. They have reported systematic changes in the statistical quantities such as the mean temperature, turbulent heat flux and turbulent Prandtl number as Pr is increased. It is further confirmed that, at high Prandtl numbers, the pressure temperature-gradient correlation is found dominant instead of the molecular dissipation as a sink term in the turbulent heat flux budget.

The Nusselt numbers calculated by the DNSs mentioned above and those of Hanratty and his colleagues (Lyons et al., 1991; Brooke, 1994; Na et al., 1998) are shown in Fig. 3. Here, Nu has been divided by $Re_b^{0.8}$ so as to compare the data at different Reynolds numbers as a function of Prandtl number. All the results are in good agreement with the values recommended by Kays & Crawford (1980).

An interesting attempt at high Pr DNS has been made by Yano & Kasagi (1997). The idea they pursued was that, since

only the spectra of thermal turbulence are broadened with Pr , it would be possible to run only the simulation of thermal turbulence on a finer grid, while using the original grid sufficient for fluid turbulence. They ran DNSs of forced homogeneous isotropic turbulence with a constant temperature gradient at $Re = k^2/\nu\epsilon = 30 - 85$ and $Pr = 0.7 - 100$, and found that it is actually possible to perform DNS at a Prandtl number much larger than unity with moderate increase in computational load. This was done by employing, only for the temperature field, approximately $Pr^{3/2}$ times more grid points than those required for the velocity field.

As an example, instantaneous thermal fields at $Pr = 0.7$ and 20 are compared in Fig. 4, where the contours of square temperature gradient $G_i^2 = (\partial\theta/\partial x_i)^2$ are represented. The distribution of G_i^2 at $Pr = 0.7$ is somewhat blurred, whilst that at $Pr = 20.0$ clearly exhibits finer structures. However, both global patterns are indifferent; the fine thermal structures are

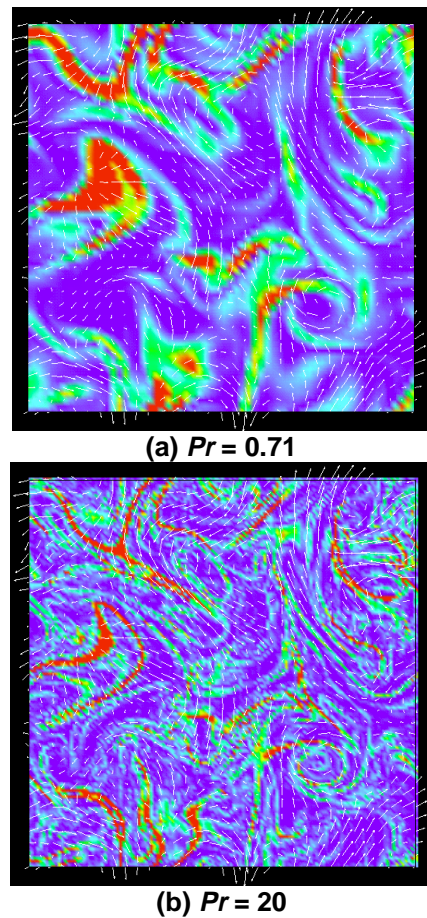


Figure 4 Instantaneous distributions of square temperature gradient at different Prandtl numbers

also associated with continuous deformation due to large-scale vortical motions. This association of the temperature gradient into a vortical motion, which is called wrapping (Guezennec et al., 1990), becomes more remarkable at higher Pr numbers. Thus, the low-wave number components of velocity fluctuation seem to cause mainly the cascade of temperature fluctuation. This qualitative understanding has been separately verified by an analysis of the transfer functions of temperature variance in wave number space. It indicates that, irrespective of Prandtl number, two close wave number modes of temperature and a lower wave number mode of velocity should be responsible for the cascade transfer in the way similar to the cascade of turbulent kinetic energy. Also note that the microscale of temperature fluctuation is found to be proportional to $Pr^{1/2}$ in good agreement with the prediction of Batchelor (1959).

Although the above method of saving grid points at high Pr has not been accessed systematically in the DNS of wall turbulence, De Angelis et al. (1997) have adopted a similar technique for a DNS of free surface turbulence with mass transfer at Schmidt numbers of 10 and 25. At these Sc numbers, they limit their simulation of mass transfer to a near-wall region at $y^+ < 43$ where significant mean gradients are expected, while solving the turbulent flow field at $y^+ \leq 171$ with the same number of grid points. Hence, a more grid density is given to the concentration field than the velocity field. They have obtained mass transfer coefficients in good accordance with laboratory experiments.

Another promising technique of simulating high Pr number thermal turbulence has been proposed by Papavassiliou & Hanratty (1997). Their method is Lagrangian simulation of the dispersion of heat markers from wall sources, with which they carry out DNSs of turbulent heat transfer at $Pr = 0.1 - 2400$. The flow field at $Re_\tau = 150$ is simulated by an Eulerian DNS with a $128 \times 65 \times 128$ grid, and the trajectories of heat markers from a wall are calculated by assuming that a marker at each time step Δt has the velocity of the fluid particle, which consists of convective and molecular effects. The convective velocity is estimated from the DNS, while the molecular diffusion is simulated by imposing a three-dimensional random walk of a Gaussian distribution with zero mean and standard deviation $\sqrt{2\Delta t / Pr}$ in wall units. They successfully observed the transfer mechanism in the close vicinity of the wall, including the wall-limiting behavior of turbulent fluxes at extremely high Pr numbers. Their results of heat transfer coefficient are also included in Fig. 3, where it is evident that they are consistent with other DNSs.

Buoyancy Effect on Turbulent Heat Transfer

Two distinct modes of forced and natural convection often appear combined together in engineering applications and

environmental flows, e.g., in heat exchangers, turbine blades, solar panels, nuclear reactors, electronic equipment and geophysical flows. Among this type of convective flows, when the mean flow is driven in the horizontal direction, it is called stratified flow, of which stratification is either stable or unstable. When unstable stratification is imposed, turbulence is enhanced, whilst under stable stratification turbulence diminishes and eventually becomes relaminarized (Narashimha & Sreenivasan, 1979; Tritton, 1988). It is also known that, under strong stratification, characteristic fluid motions generated by buoyancy, i.e., the internal gravity waves and thermal plumes, interact with turbulence (Turner, 1973). Although detailed measurements are extremely difficult, some laboratory experiments have been carried in horizontal boundary layer and channel flows to reveal buoyancy effects on wall turbulence (Kasagi and Hirata, 1977; Komori et al, 1983; Fukui et al., 1983, 1991).

On the other hand, upward flows along heated and cooled vertical walls are respectively referred to as aiding and opposing flows depending upon the combination of the directions of flow and buoyancy. The experiments in literature show that in the aiding flow both the turbulence and the heat transfer rate are suppressed in spite of the increased mean flow velocity, whereas in the opposing flow the turbulence activity is enhanced with the mean velocity decreased (Jackson et al., 1989).

The buoyancy effects on turbulence and heat transfer have been intensively studied by DNSs, but in many cases in homogeneous shear flows with stable stratification (Gerz et al., 1989; Holt et al., 1992; Jacobitz et al., 1997). There are only a few DNSs of wall turbulence under stable (Coleman et al., 1992; Iida et al., 1997a) and unstable (Domaradzki & Metcalfe, 1988; Iida & Kasagi, 1997) stratification, and of the aiding and opposing flows (Kasagi & Nishimura 1997).

Hereafter, two kinds of channel flows are examined. The first one is a fully developed horizontal turbulent channel flow (Iida & Kasagi, 1997; Iida et al., 1997a), and the second one is the vertical channel (Kasagi & Nishimura 1997); in both cases the walls are kept at different, but isothermal temperatures. In the former the buoyancy due to stable or unstable density stratification does not affect directly the mean field, but only through the turbulent fluctuations, whereas in the latter the buoyancy force has a substantial effect on the mean force balance. This distinct mechanisms can be inferred by examining the transport equations of the second-order moments of turbulent fluctuations (Launder, 1978).

The geometry and coordinate system of horizontal channel flow are shown in Fig. 5. The Reynolds number $Re_\tau (= u_\tau \delta \nu)$ was kept at 150, while the Prandtl number was assumed to be 0.71. In the DNS of the unstably stratified flow, the Grashof

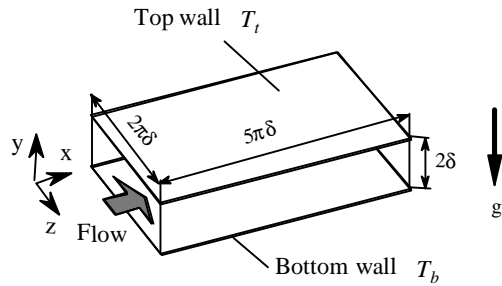


Figure 5 Geometry and coordinate system of horizontal channel flow

number Gr ($= g\beta(\Delta T)(2\delta)^3/\nu^2$), which is based on the temperature difference between the two walls $\Delta T (= T_h - T_c)$ and the channel width 2δ , was varied from 0 to -4.8×10^6 . On the other hand, in the stably stratified flow, Gr was varied from 0 to 2×10^7 . All of these DNSs at different Grashof numbers are calculated by a pseudo-spectral method (Kim et al., 1987) on a relatively coarse grid, i.e., $64 \times 49 \times 64$ in the x -, y - and z -directions, respectively. These results are mainly used to examine qualitatively the dependence of the flow characteristics on the imposed buoyancy. In order to assess the numerical accuracy, a fine grid of $128 \times 97 \times 128$ is used in some typical cases.

Figures 6 and 7 show the changes in the normalized friction coefficient and Nusselt number versus the bulk Richardson number $Ri_b (= Gr/Re_b^2)$, respectively. In Fig. 7, two kinds of Nusselt numbers are plotted, i.e., Nu^* represents the dimensionless heat transfer coefficient based on the temperature difference between the two walls, while Nu is based on the wall to bulk mean temperature difference. Under unstable stratification, as the Richardson number is increased, the friction coefficient first decreases and takes a minimum around $Ri_b = 0.05$. This is because the buoyancy-driven secondary flow deteriorates the near-wall turbulence and increases the thickness of the viscous sublayer as discussed later. When Ri_b further increases, C_f starts to increase because the contribution of the secondary flow to the momentum transfer is more enhanced. On the other hand, the Nusselt number Nu simply increases with Ri_b , although it shows a plateau around $Ri_b = 0.05$. In the stably stratified channel, both C_f and Nu decrease markedly with increasing Ri_b . It has been confirmed separately that, when Ri_b reaches 0.54, the flow becomes almost relaminarized (Iida et al., 1997a). It is interesting that in both cases of stratification the buoyancy force causes a larger change in the Nusselt number than in the skin friction coefficient. Note also that the DNSs agree well with previous experimental results (Fukui et al., 1983).

The logarithmic plots of the mean velocity and temperature

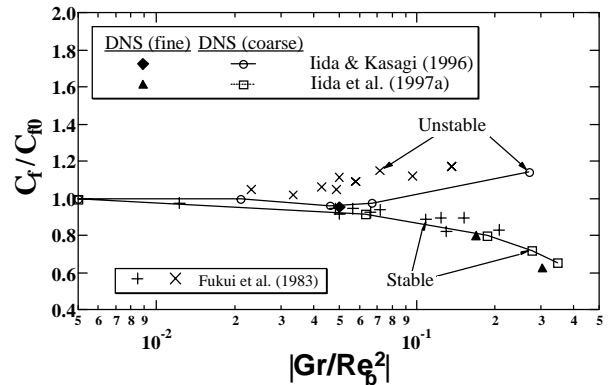


Figure 6 Dependence of the normalized skin friction coefficients on bulk Richardson number

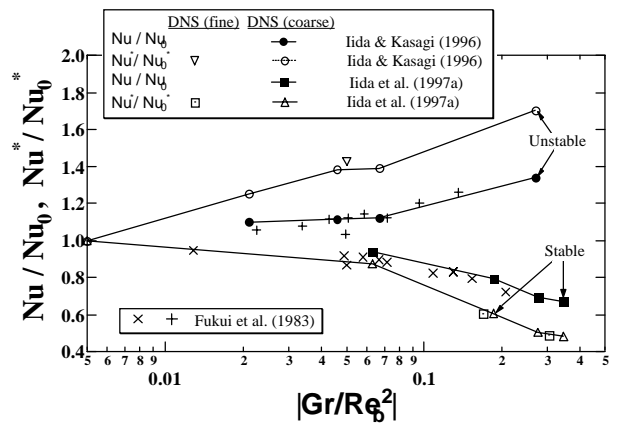


Figure 7 Dependence of the normalized Nusselt numbers on bulk Richardson number

distributions are shown in Figs. 8 and 9, respectively. In all unstably stratified cases, the mean velocity in the channel central region tends to decrease. However, at $Gr = -1.3 \times 10^6$, the mean velocity increases in the buffer as well as logarithmic regions; this is associated with the aforementioned decrease in the friction coefficient. Although not shown here, this increase of the mean velocity is mainly due to the reduction of the Reynolds shear stress in the region at $y^+ < 30$. When the magnitude of Gr is further increased to $Gr = -4.8 \times 10^6$, the mean velocity decreases in almost all regions. As a result, the shear production of Reynolds shear stresses decreases over the entire channel cross section, and both the pressure and turbulent diffusions become more important. This is similar to the transport mechanism in the wall turbulence with a reduced shear rate (Kuroda et al., 1995; Hunt, 1984).

In the stably stratified channel, the mean velocity tends to increase in the region $y^+ > 10$. Namely, the thickness of the buffer region increases and the logarithmic region disappears. This should be because, under stable stratification, the

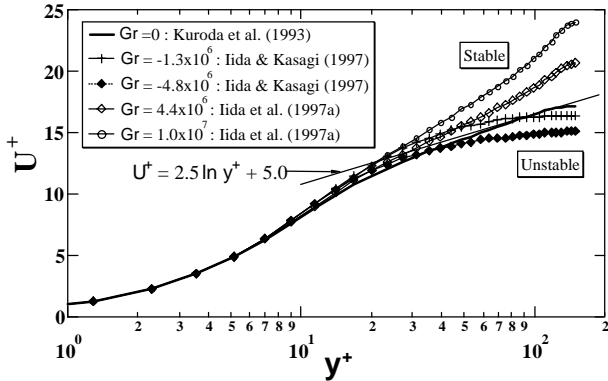


Figure 8 Logarithmic plot of the mean velocity

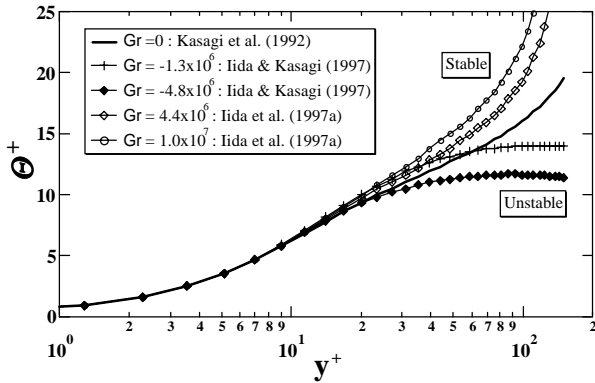


Figure 9 Logarithmic plot of the mean temperature

turbulence structure becomes smaller and indifferent to the distance from the wall, i.e., Z-less scaling of the turbulence (Stull, 1988), and the assumption of the standard logarithmic law becomes invalid. The disappearance of the logarithmic region is also confirmed in the DNS of a rotating pipe (Orlandi & Fatica, 1997), and this fact supports analogy between the effects of rotation and stratification (Bradshaw, 1969).

The effects of stratification on the mean temperature distributions are similar to those observed in the mean velocity profiles, so that the similarity between the turbulent heat and momentum transfer is almost valid even in the horizontally stratified flows. However, the change in the mean temperature profile is more marked in the channel central region, where the gradient Richardson number takes the largest value.

A typical example of instantaneous velocity vector and temperature distributions in a cross-stream plane of the unstable channel flow at $Gr = -1.3 \times 10^6$ is shown in Fig. 10; this is the case in which the skin friction coefficient is found to decrease compared to the case without buoyancy. Both thermal plumes and quasi-streamwise vortices can be clearly identified. The large-scale downward and upward plumes

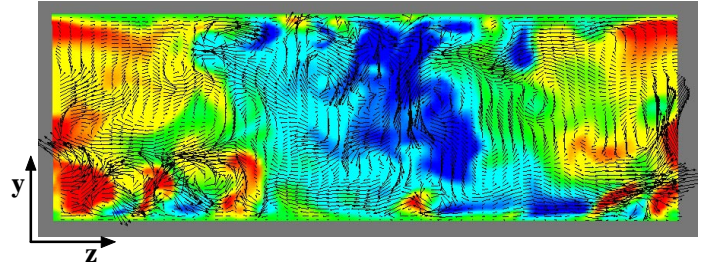
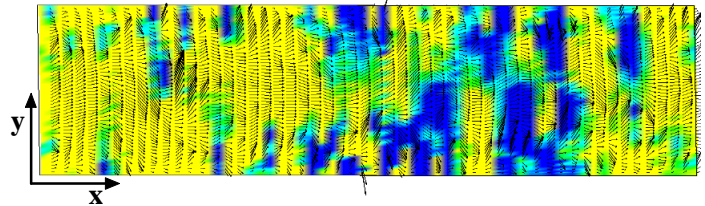
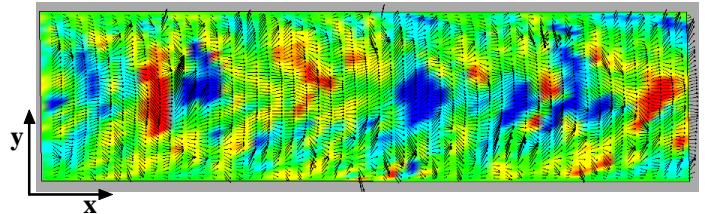


Figure 10 Instantaneous velocity vectors and temperature fluctuations in the y - z plane ($\Delta y^+ \times \Delta z^+ = 300 \times 943$) of the unstably stratified channel ($Gr = -1.3 \times 10^6$): blue to red; $\theta/\Delta T = -0.15$ to 0.15

are seen at the center and two sides of Fig. 10. The thermal plumes as large as the width of the channel height emerge from the near-wall region. The quasi-streamwise vortices seem to be swept out by the spanwise flow component induced by the plumes and concentrated into the confined regions where another thermal plume emerges. Note that the turbulent skin friction is closely associated with the quasi-streamwise vortices (Robinson, 1991). Hence, the viscous sublayer thickens due to the plumes and the skin friction coefficient decreases. However, the large-scale plumes are also effective in transporting heat between two walls as shown in Fig. 10, so that the decrease of the Nusselt number should not appear despite the increased thickness of the



(a) With pressure fluctuations: blue to green, $p^+ = -4$ to 0



(b) With temperature fluctuations: blue to red, $\theta/\Delta T = -0.15$ to 0.15

Figure 11 Instantaneous velocity vectors ($U + u, 12v$) in the x - y plane ($\Delta x^+ \times \Delta y^+ = 2356 \times 300$ with the x -axis compressed to one half) of the stably stratified channel ($Gr = 1 \times 10^7$)

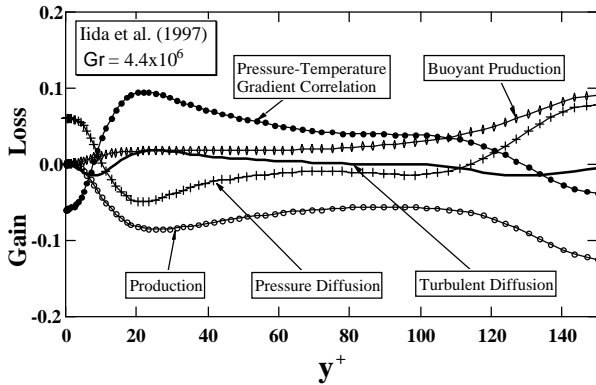


Figure 12 Budget of the wall-normal turbulent heat flux

sublayer. The deterrence of the near-wall turbulence due to the secondary flow is also observed in the turbulent channel flow under system rotation (Nishimura & Kasagi, 1996; Bech & Andersson, 1996).

The stable stratification generates the unique flow structures, which contribute little to heat transfer. Figure 11(a) shows an example of velocity vectors and pressure contour in the x - y plane at $Gr = 1 \times 10^7$, while Fig. 11(b) shows temperature fluctuations at the same instance. In Fig. 11(a), the wave-like motions are clearly observed in the channel central region. The characteristics of this fluid motion are studied statistically by the phase difference between the streamwise and wall-normal velocity fluctuations, which shifts from zero to $\pm\pi/2$. They are the so-called internal gravity waves, because the phase difference between the temperature and wall-normal velocity fluctuations also becomes $\pm\pi/2$ (Stull, 1987; Komori et al, 1983) and their correlation diminishes to almost zero in the channel central region. Figure 11(a) also shows that the elongated low-pressure regions are formed between the wall and the crest of the internal waves. These low-pressure regions correspond to the streamwise vortices, which are extended down to the wall and entrained into the crest of the waves. The internal gravity waves and streamwise vortices interact through pressure, by which the turbulent kinetic energy is exchanged. However, it is found from Fig. 11(b) that the intensive temperature fluctuations, which are associated with the internal gravity waves, are not in direct contact with the heated and cooled wall, but confined in the channel central region. Hence, the heat transfer between the two walls is seriously impeded. In the stably stratified channel, the dynamically important internal gravity waves do not contribute to the heat transfer and works substantially as an adiabatic layer.

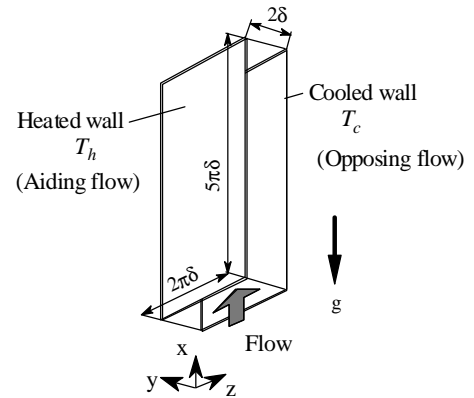


Figure 13 Flow geometry and coordinate system for the vertical channel

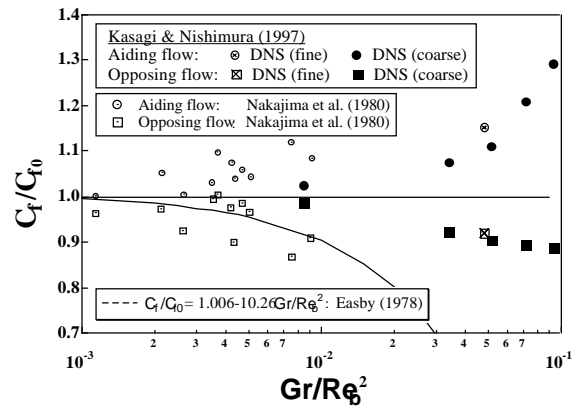


Figure 14 Dependence of normalized friction coefficient on buoyancy

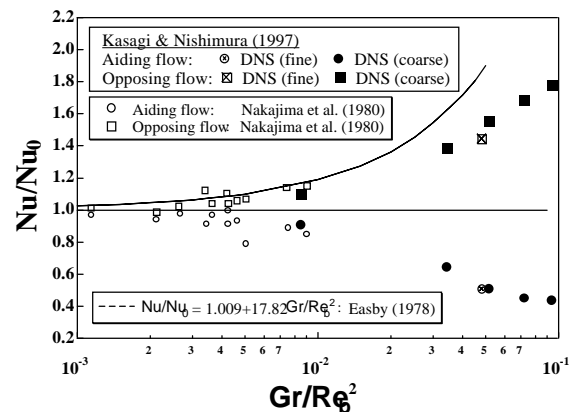


Figure 15 Dependence of normalized Nusselt number on buoyancy

The effects of stable buoyant force on the turbulent heat transfer are also observed in the budget terms of the wall-normal turbulent heat flux, i.e., $\overline{v\theta}$, as shown in Fig. 12. In the budget of $\overline{v\theta}$ (<0), the dominant source term is the

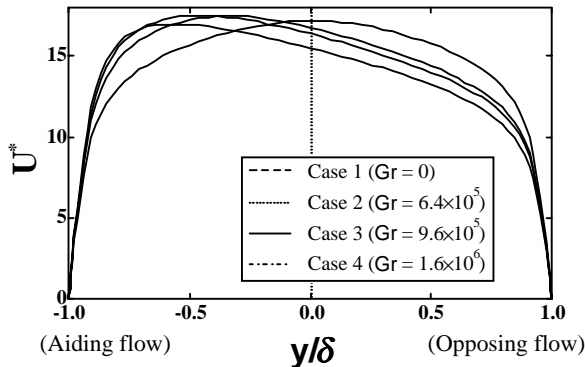


Figure 16 Mean velocity profile in global coordinates

production term due to the wall-normal velocity fluctuation and the mean temperature gradient, while the pressure-scrumbling term (pressure-temperature gradient correlation) contributes to destruction of $\overline{v\theta}$. When stable density stratification is imposed, the buoyant production, $-g\beta\theta^2$, appears in the budget of $\overline{v\theta}$. It is evident in Fig. 12 that this buoyancy term takes the largest value in the channel central region, where the pressure diffusion term also works as an additional sink. Hence, the turbulent heat flux is damped significantly there. This fact is associated with the above mentioned internal gravity waves.

The buoyancy effect appears in an essentially different manner in the vertical channel flow. The flow geometry and coordinate system are shown in Fig. 13. DNSs at different Grashof numbers were carried out on coarse ($64 \times 49 \times 64$) as well as fine ($128 \times 97 \times 128$) grids. The relative changes of the friction coefficient and the Nusselt number are shown in Figs. 14 and 15, respectively. They are calculated by using the following equations:

$$Nu = 2q_w \delta / (\langle T \rangle - T_w) / \lambda, \quad (1)$$

$$C_f = 2\tau_w / \rho \langle U \rangle^2, \quad (2)$$

where $\langle \rangle$ denotes a bulk-averaged quantity over d , which is the interval from the wall to the maximum velocity location. It is evident that C_f increases in the aiding flow (on the heated wall), while decreased in the opposing flow (on the cooled wall), with increasing Gr/Ri_b^2 . However, Nu exhibits an inverse trend; it is decreased and increased in the aiding and opposing flows, respectively. These facts are in good agreement with the results found in the previous investigations, although the empirical formula of Easby (1978) seems to over predict the buoyancy effect at large values of Gr/Re_b^2 .

The mean velocity profile in the global coordinates is shown in Fig. 16. It is evident that the velocity profile becomes more asymmetric as Gr increases. The peak

location shifts toward the aiding-flow side, where the mean velocity is accelerated by the buoyant force, and hence the skin friction coefficient increases. The decrease of Nusselt number is also associated with the shift of the maximum mean velocity toward the aiding flow side. On the opposing flow side, the opposite changes take place.

In Figs. 17 and 18, C_f and Nu in both the vertical and horizontal channels are plotted against the bulk Reynolds number Re_b . Note that the bulk Reynolds number is now based on the distance from the location of the maximum mean velocity to the wall. The results of the opposing and aiding flows agree fairly well with the standard correlation or experimental data, i.e., Dean (1978), Patel & Head (1969) and Kays & Crawford (1980). Hence, the relaminarization in the aiding flow should be due to the decreased bulk Reynolds number, while the opposing flow should be interpreted as a higher bulk Reynolds number flow. On the other hand, the results of both stable and unstable density stratification deviate markedly from the standard correlation, because the buoyancy force and the associated secondary flow alter substantially the

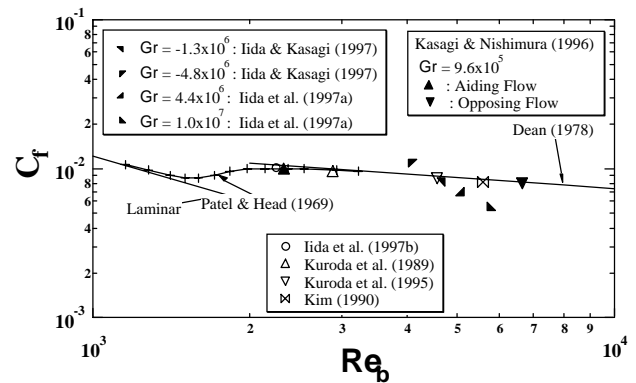


Figure 17 Skin friction coefficient versus bulk Reynolds number

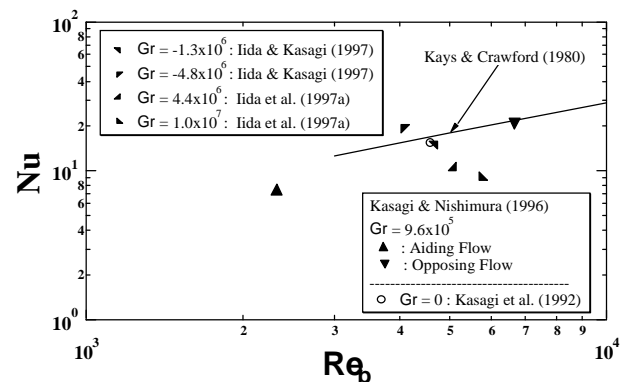


Figure 18 Nusselt number versus bulk Reynolds number

turbulence structures and transport mechanism.

SMART CONTROL OF TURBULENT HEAT TRANSFER

Control of turbulence and heat transfer has been one of the central issues in modern scientific, engineering and environmental research efforts. Its potential benefits can be easily recognized if one thinks about the significance of the artificial manipulation of turbulent drag, noise, heat transfer as well as chemical reaction, to name a few. Over the several decades, many intensive investigations have been undertaken focusing on possible heat transfer control techniques. Although there is a considerable degree of knowledge on such methods as roughness/grooves, twisted tapes, blowing/suction and polymer additives, the major difficulty exists in controlling momentum and heat transfer independently. Namely, most heat transfer enhancement techniques are associated with an excess amount of pressure loss penalty, and the real enhancement is usually limited to a low Reynolds number regime. An exception is the spirally fluted tube (Yampolsky, 1979), in which the swirling velocity caused by the flute on the inner tube surface maintains core-region turbulence low while enhancing heat transfer of high Pr number fluids with the secondary flow in the flute cavity (Cheah et al., 1993). Dissimilarity between heat and momentum transfer (Inaoka et al., 1998) does not take place easily without a particular flow arrangement, which may not always be possible in real applications.

Efforts are now directed toward to active or interactive control schemes, particularly those exploiting emerging micromachining technology, called microelectromechanical systems (MEMS) (Moin & Bewley, 1994; Ho & Tai, 1996; Jacobson & Reynolds, 1993). The turbulent structures in real flows are very small in size, typically several hundred microns in width and a few mm in length in wall turbulence. Their lifetime is also very short. In the past, direct manipulation of these structures was very difficult, but is now expected to become possible with miniature sensors and actuators of micron size fabricated by MEMS. This new technology offers a batch production process, through which micromechanical parts are produced in large quantities. A MEMS controller unit, with its integrated mechanical parts and IC, will be able to sense the physical world, process the information, and then manipulate the physical phenomena through actuators. From this viewpoint, studies of active turbulence control now begin to use DNSs extensively for analyzing the effectiveness of proposed control algorithms (Choi et al., 1994; Moin & Bewley, 1995; Satake & Kasagi, 1997; Lee et al., 1997) to lead the future development of MEMS controllers and systems. Two examples of latest DNSs are introduced below.

Endo et al. (1999) assumes an array of micro deformable actuators on a wall of turbulent channel flow for possible drag reduction and heat transfer augmentation as shown in Fig. 19.

Choi et al. (1994) employed local blowing and suction, based on the instantaneous wall-normal velocity near the wall, and obtained about 30% drag reduction by interfering with the longitudinal vortices. Similarly, the velocity at the center of each actuator is determined in the same manner as follows:

$$v_w^{n+1} = -\alpha v_w^n + \beta (v_s^n - \langle v_s^n \rangle) \quad (3)$$

Here, v_s is the wall-normal velocity detected at $y/\delta = 0.1$ ($y^+ \sim 15$), while v_w is the velocity of the center of each wall actuator, of which shape is given as a Gaussian distribution. The bracket $\langle \chi \rangle$ denotes an ensemble average of quantity χ in the x - z plane at each time step n . The first term on the RHS of Eq. (3) is a damping term to suppress excessive wall deformation. When β is negative, the wall deformation would decelerate the fluid movement near the wall.

The size of each actuator is to be optimized so that it would give the best control result with the least number of actuators. It is, however, anticipated to be on the order of the size of the longitudinal vortices, which play a primary role in momentum and heat transport in wall turbulence (Kasagi et al., 1995). A time trace of the relative change in pressure loss is shown in Fig. 20, where the actuator is assumed to have a size of 50×7.3 wall units in the x - and z -directions, respectively, with $\alpha = 2$

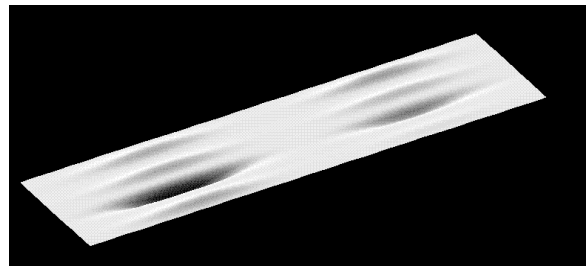


Figure 19 Arrayed micro actuators (2x4) on a wall for turbulence control

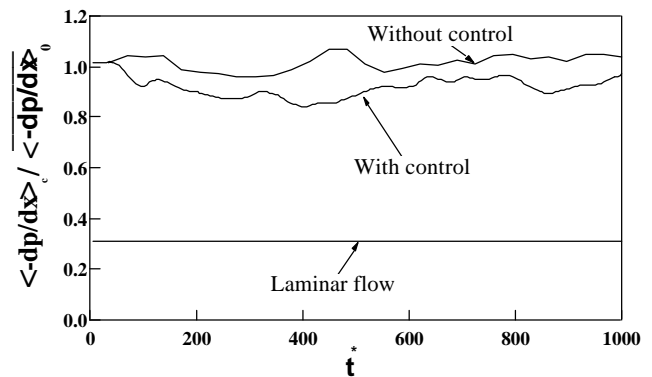


Figure 20 Time trace of normalized pressure gradient in channel flow

and $\beta = -1$. It is evident that the array of elongated micro-actuators with a simple control algorithm works efficiently for drag reduction.

In a recent experimental investigation of turbulent heat transfer in a gas-particle two-phase flow, Hishida and Maeda (1994) tried to exploit soft magnetic particles made of nickel-zinc-ferrite, which lost magnetism when their temperature exceeded the Curie temperature. They were successful in enhancing the local heat transfer coefficient as much as 60%. This idea can be conceptually extended to fabrication of smart particles with the aid of MEMS. Hence, DNS of a particle-laden channel flow has been made to further explore the possibility of enhancing heat transfer with intelligent particles by Arai et al. (1998). The particles are endowed with a body force on-off switching depending on temperature.

The motion of each particle is calculated in a Lagrangian frame by using the equation of motion:

$$\frac{du_{p,i}^+}{dt^+} = \frac{1}{\tau_p^+} (u_{f,i}^+ - u_{p,i}^+) + a_e^+(\theta_p^*) \delta_{i,2} \quad (4)$$

where all variables are made dimensionless with the wall variables, and subscripts f, p and 2 denote fluid, particle and the

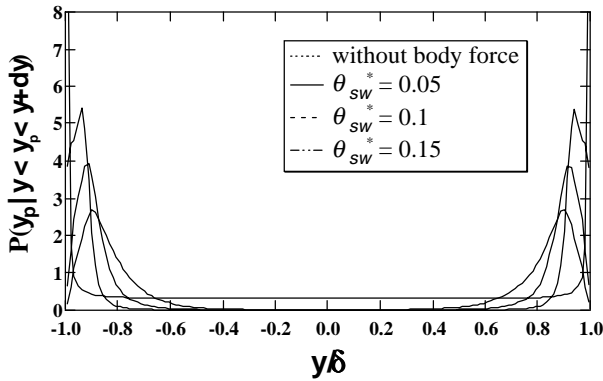


Figure 21 Particle Number Density Distribution

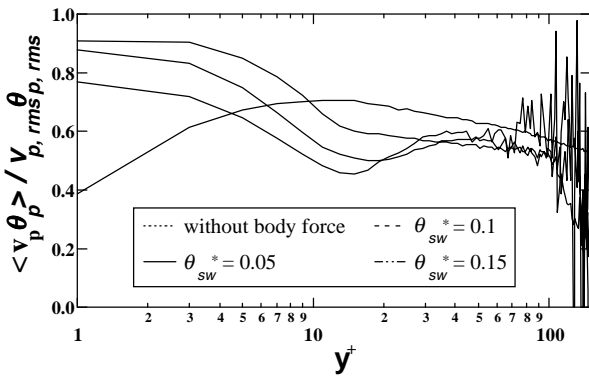


Figure 22 Relative Correlation Coefficient of Wall-Normal velocity and Temperature Fluctuations of Particle

wall-normal direction, respectively. Note also that the first and second terms on the RHS of Eq. (4) are the Stokes drag force and the virtual body force, respectively. It is assumed that the flow field is affected by the particles only thermally, but not dynamically. The heat transfer coefficient around the particle is given by the empirical formula of Ranz (1952). The virtual force term in Eq. (4) is a function of the temperature normalized by the temperature difference between two channel walls as follows:

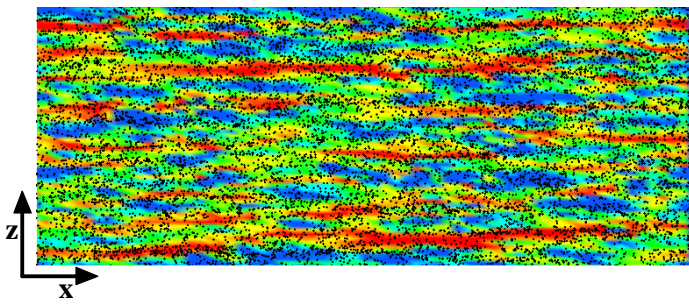
$$a_e^+(\theta_p^*) = \begin{cases} -0.5 & (0 \leq \theta_p^* \leq \theta_{sw}^*) \\ +0.125 & (\theta_{sw}^* < \theta_p^* < 0.5) \end{cases} \quad (5)$$

where θ_p^* is the threshold temperature, at which the body force changes its acting direction. Namely, the particle is pushed away from the wall in the near-wall region, whilst attracted toward the wall in the central region of the channel. The magnitude of body force is assumed to be on the same order as that of the Stokes drag, so that the work of driving the particles should be small enough to assure the net heat transfer augmentation.

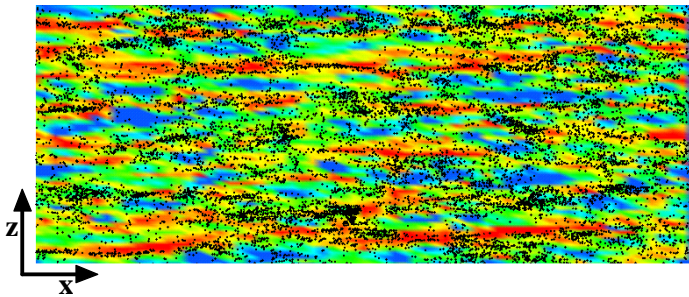
The particles' conditions are given by referring to Hishida and Maeda: i.e., the density ratio, $\rho_p/\rho_f = 4460$; the specific heat ratio, $c_p/c_f = 0.76$; the relaxation time constant of particle, $\tau_p^+ = (\rho_p/\rho_f)/(d_p^{+2}/18) = 5.2$; the thermal relaxation time constant of particle, $\tau_\theta^+ = 3(c_p/c_f) \tau_p^+ Pr/Nu_p = 4.2$; the dimensionless particle diameter, $d_p^+ = 0.1448$; the mass loading ratio, $\phi_m = 0.069$; $Re_\tau = 150$, and $Pr = 0.71$. The threshold temperature is changed as $\theta_p^* = 0.05, 0.1$ and 0.15 , which roughly correspond to the mean temperatures at $y^+ = 2.5, 5$ and 10 , respectively.

As a result, it is found that the heat transfer coefficient is increased by 3.3% by simply introducing particles, but even by 16%, 11.7%, and 9% when $\theta_p^* = 0.05, 0.1$ and 0.15 , respectively. The probability density of particles' location is shown in Fig. 21. The peak concentration moves away from the wall as θ_p^* is increased, otherwise it exists on the wall surface. The contribution of these intelligent particles to heat transfer can be evaluated in Fig. 22, where the correlation coefficient between the wall-normal velocity and temperature fluctuations of the particle is compared with that of the inactive particles. It is evident that the correlation is significantly improved by the body force at $y^+ < 10$, where the conductive heat flux dominates the turbulent heat flux. Note that the magnitude of heat transfer augmentation should increase with the mass loading ratio.

Instantaneous flow fields are shown in Fig. 23. With virtual body force, the distribution of particle is no longer uniform, but exhibits clustering along the high-temperature (low-speed) streaks (Iritani et al., 1984) in the viscous wall region. Thus, the particles transport heat outside the conductive sublayer more efficiently. Since the particle's diameter is assumed to be very small in these simulations, it is expected



(A) without body force



(b) with body force ($\theta_{sw} = 0.05$)

Figure 23 Particle concentration at $y^+ < 7$ and temperature fluctuation at $y^+ = 2.9$ ($\Delta x^+ \times \Delta y^+ = 2356 \times 300$): blue to red corresponds to low to high temperatures

that its dynamical effect is mainly dissipative so that the turbulent friction drag would not increase, but may decrease. This point remains to be fully resolved in the future work.

As modern knowledge on the structure of turbulent flow is successfully exploited in choosing the effective mode of manipulation in the above DNSs, an attempt at controlling the turbulent heat transfer is based on empiricism or intuition in many cases. Hence, it is a desirable option to cast this problem into the framework of optimal control theory; i.e., the spatio-temporal distribution of control input should be optimized in the sense that the maximum control performance is achieved with the least control input energy. Recently, by simplifying the optimal control theory (Abergel & Temam, 1990), Choi et al. (1993b) devised a suboptimal feedback control algorithm for the Navier-Stokes equations and applied it to the stochastic Burgers equation. Later, this suboptimal control scheme was successfully used in optimizing proposed control modes for drag reduction in channel flows by Choi (1995), Moin & Bewley (1995), and Satake & Kasagi (1997). Different types of active feedback control algorithms based upon adaptive schemes and dynamical systems theory are also being studied (Moin & Bewley, 1994). For instance, a nonlinear adaptive

algorithm, called neural networks, has a wide range of applicability (Jacobson & Reynolds, 1993; Lee et al., 1997), since it does not require precise mathematical description of the system nor empirical knowledge on physical mechanisms. These new proposals for smart turbulent heat transfer control should also be tested and evaluated through the further use of DNSs.

CONCLUDING REMARKS

Direct numerical simulation offers valuable numerical experiments for turbulence heat transfer research. With high performance computers, reliable numerical methods and efficient post-processing environment, a variety of applications of DNS are possible. In particular, one can extensively study the turbulence dynamics and transport mechanism by visualizing any of physical variables in space and time. It is also possible to establish detailed database of various turbulence statistics in turbulent transport phenomena, while systematically changing important flow and scalar field parameters.

The present paper has illustrated such novelties of DNS by introducing several examples of recent studies. An effort to reveal the Prandtl number effect on turbulent heat transfer is sketched with the new techniques developed for making DNS over a wide Prandtl number range possible. Both methods of saving grid points and Lagrangian particle tracking are very useful in the future research on turbulent heat and mass transfer. The complex buoyancy effects on turbulent transport are systematically investigated in a series of DNSs of horizontal and vertical channel flows. It has been observed that the buoyancy effect appears distinctly depending upon the directional alignment of the buoyant force and the mean flow. In the vertical flow, the buoyancy can be interpreted as an increased or decreased Reynolds number effect, whilst in the horizontal flow it can cause substantial alternation in the turbulence structures and transport mechanism so that the resultant heat transfer coefficient would behave in a much more complex manner. The thermal plumes and internal gravity waves characteristic of these flows play an important role in the interaction with the quasi-coherent structures of wall turbulence.

Finally, DNSs have been introduced to the work on active turbulence and heat transfer control, in which an array of micro deformation actuators on a wall surface or intelligent micro particles are tested. It is shown that these control schemes possibly bring about notable turbulent friction drag reduction and heat transfer enhancement. A perspective view is given that DNS will be even more useful in evaluating future turbulence control methodologies based on new algorithms such as optimum control theory and neural networks. These simulations

have been triggered by the rapid development of MEMS technology, but hopefully future DNSs will lead further development of MEMS-based controller units integrating micro sensors, micro actuators and IC. There are yet many complex but important problems of turbulent transport such as multiphase flows and those with chemical reactions, of which DNSs should be challenged. Thus, there is no doubt that DNS will serve continuously as a powerful tool for fundamental turbulence research in the coming century.

ACKNOWLEDGEMENTS

The authors are grateful to Professors T. J. Hanratty, H. Kawamura and Y. Nagano for offering their DNS data to the present work.

REFERENCES

- Abergel, F., and Temam, R., 1990, "On Some Control Problems in Fluid Mechanics," *Theor. Comput. Fluid Dyn.*, Vol. 1, pp. 303-325.
- Adam, Y., 1977, "High Accurate Compact Implicit Methods and Boundary Conditions," *J. Comput. Phys.*, Vol. 24, pp. 10-22.
- Arai, Y., Mizuya, T., Kasagi, N., and Suzuki, Y., 1998, "Numerical Simulation of Turbulent Heat Transfer Controlled by Dispersed Solid Particles," *Proc. 35th Natl. Heat Transfer Symp. Japan*, Nagoya, Vol. 3, pp. 775-776.
- Batchelor, G. K., 1959, "Small-Scale Variation of Convected Quantities Like Temperature in Turbulent Fluid: Part 1. General Discussion and the Case of Small Conductivity," *J. Fluid Mech.*, Vol. 5, pp. 113-133.
- Bech, K. H., and Andersson, H. I., 1996, "Secondary Flow in Weakly Rotating Turbulent Plane Couette Flow," *J. Fluid Mech.*, Vol. 317, pp. 195-214.
- Bradshaw, P., 1969, "The Analogy Between Streamline Curvature and Buoyancy in Turbulent Shear Flow," *J. Fluid Mech.*, Vol. 36, pp. 177-191.
- Brooke, J. W., 1994, "Transport Processes in a Direct Numerical Simulation of Turbulent Channel Flow," Ph. D. thesis, University of Illinois, Urbana, Illinois.
- Canuto, C., Hussaini, M. Y., Quarteroni, A., and Zang, T. A., 1987, "Spectral Method in Fluid Dynamics," Springer, Berlin.
- Carlson, H. A., and Lumley, J. L., 1996, "Active Control in The Turbulent Wall Layer of a Minimal Flow Unit," *J. Fluid Mech.*, Vol. 329, pp. 341-371.
- Cheah, S. C., Cheng, L., Cooper, D., and Launder, B. E., 1993, "On the Structure of Turbulent Flow in Spirally Fluted Tubes," *5th IAHR Conf. Refined Flow Modelling & Turbulence Measurement*, Paris.
- Choi, H., 1995, "Suboptimal Control of Turbulent Flow Using Control Theory," *Proc. Int. Symp. Math. Model. Turbulent Flows*, Tokyo, pp. 131-138.
- Choi, H., Moin, P., and Kim, J., 1993a, "Direct Numerical Simulation of Turbulent Flow over Riblets," *J. Fluid Mech.*, Vol. 255, pp. 503-539.
- Choi, H., Moin, P., and Kim, J., 1994, "Active Turbulence Control for Drag Reduction in Wall-Bounded Flows," *J. Fluid Mech.*, Vol. 262, pp. 75-110.
- Choi, H., Temam, P., Moin, P., and Kim, J., 1993b, "Feedback Control for Unsteady Flow and Its Application to The Stochastic Burgers Equation," *J. Fluid Mech.*, Vol. 253, pp. 509-543.
- Chorin, A. J., 1969, "On the Convergence of Discrete Approximations to the Navier-Stokes Equations," *Math. Comput.*, Vol. 23, pp. 341-353.
- Chu, D. C., and Karniadakis, G. E., 1993, "A Direct Numerical Simulation of Laminar and Turbulent Flow over Riblet-Mounted Surfaces," *J. Fluid Mech.*, Vol. 250, pp. 1-42.
- Coleman, G. N., Ferziger, J. H., and Spalart, P. R., 1992, "Direct simulation of the Stably Stratified Turbulent Ekman Layer," *J. Fluid Mech.*, Vol. 244, pp. 677-712.
- De Angelis, V., Lombardi, P., and Banerjee, S., 1997, "Numerical Investigation of Turbulent Heat Transfer Mechanisms at a Gas-Liquid Interface," *Proc. 11th Symp. Turbulent Shear Flows*, Grenoble, Vol. 3, pp. 27.24-27.29.
- Dean, R. B., 1978, "Reynolds Number Dependence of Skin Friction and Other Bulk Flow Variables in Two-Dimensional Rectangular Duct Flow," *ASME J. Fluids Eng.*, Vol. 100, pp. 215-223.
- Domaradzki, J. A., and Metcalfe, R. W., 1988, "Direct Numerical Simulation of the Effects of Shear on Rayleigh-Benard Convection," *J. Fluid Mech.*, Vol. 193, pp. 499-531.
- Easby, J. P., 1978, "The Effect of Buoyancy on Flow and Heat Transfer for a Gas Passing Down a Vertical Pipe at Low Turbulent Reynolds Number," *Int. J. Heat Mass Transfer*, Vol. 21, pp. 791-801.
- Elghobashi, S., and Truesdell, G. C., 1993, "On the Two-Way Interaction Between Homogeneous Turbulence and Dispersed Solid Particles. 1: Turbulence Modification," *Phys. Fluids*, Vol. A5, pp. 1790-1801.
- Endo, T., Kasagi, N., and Suzuki, Y., 1998, "Feedback Control of Wall Turbulence with Wall Deformation," to be presented at *1st Int. Symp. Turbulence & Shear Flow Phenomena*, Santa Barbara, CA, 1999.
- Fogelson, A. L., and Peskin, C. S., 1988, "A Fast Numerical Method for Solving the Three-Dimensional Stokes Equations in the Presence of Suspended Particles," *J. Comput. Phys.*, Vol. 79, pp. 50-69.
- Fukui, K., Nakajima, M., and Ueda, H., 1983, "A Laboratory Experiment on Momentum and Heat Transfer in the

Stratified Surface Layer," *Quart. J. R. Met. Soc.*, Vol. 109, pp. 661-676.

Fukui, K., Nakajima, M., and Ueda, H., 1991, "Coherent Structure of Turbulent Longitudinal Vortices in Unstably-Stratified Turbulent Flow," *Int. J. Heat Mass Transfer*, Vol. 34, No. 9, pp. 2373-2385.

Gavrilakis, S., 1992, "Numerical Simulation of Low-Reynolds-Number Turbulent Flow Through a Straight Square Duct," *J. Fluid Mech.*, Vol. 244, pp. 101-129.

Gerz, T., Schumann, U., and Elghobashi, S. E., 1989, "Direct Numerical Simulation of Stratified Homogeneous Turbulent Shear Flows," *J. Fluid Mech.*, Vol. 200, pp. 563-594.

Guezennec, C., Stretch, D., and Kim, J., 1990, "The Structure of Turbulent Channel Flow with Passive Scalar Transport," *Proc. CTR Summer Program, Stanford University*, pp. 127-138.

Hirsh, R. S., 1977, "High Order Accurate Difference Solutions of Fluid Mechanics Problems by a Compact Differencing Technique," *J. Comput. Phys.*, Vol. 19, pp. 90-109.

Hishida, K., and Maeda, M., 1994, "Enhancement and Control of Local Heat Transfer Coefficients in a Gas Flow Containing Soft Magnetic Particles," *Exp. Heat Transfer*, Vol. 7, pp. 55-69.

Ho, C.-M., and Tai, Y.-C., 1996, "Review: MEMS and Its Applications for Flow Control," *ASME J. Fluids Eng.*, Vol. 118, pp. 437-447.

Holt, S. E., Koseff, J. R., and Ferziger, J. H., 1992, "A Numerical Study of the Evolution and Structure of Homogeneous Stably Stratified Sheared Turbulence," *J. Fluid Mech.*, Vol. 237, pp. 499-539.

Hunt, J. C. R., 1984, "Turbulence Structure in Thermal Convection and Shear-Free Boundary Layers," *J. Fluid Mech.*, Vol. 138, pp. 161-184.

Iida, O., and Kasagi, N., 1997, "Direct Numerical Simulation of Unstably Stratified Turbulent Channel Flow," *ASME J. Heat Transfer*, Vol. 119, pp. 53-61.

Iida, O., Kasagi, N., and Nagano, Y., 1997a, "The Effect of Stable Density Stratification on the Dynamics of Turbulent Channel Flow," *Proc. 11th Symp. Turbulent Shear Flows, Grenoble*, pp. 20.1-20.6.

Iida, O., Ohtuka, A., and Nagano, Y., 1997b, "The Drag Reduction Mechanisms in the Retransition of Turbulent Channel Flow," *Proc. 2nd Int. Symp. Turbulence, Heat & Mass Transfer, Delft*, pp. 209-218.

Inaoka, K., Yamamoto, J., and Suzuki, K., 1998, "Dissimilarity Between Heat Transfer and Momentum Transfer in a Disturbed Turbulent Boundary Layer with Insertion of a Rod," *2nd EF Conf. Turbulent Heat Transfer, Manchester*, Vol. 1, pp. 4.3-4.14.

Iritani, Y., Kasagi, N. and Hirata, M., 1984, "Heat Transfer Mechanism and Associated Turbulence Structure in a Near-Wall Region of a Turbulent Boundary Layer," *Turbulent Shear Flows IV*, L. J. S. Bradbury et al., eds., Springer, Berlin, pp. 223-234.

Jackson, J. D., Cotton, M. A., and Axcell, B. P., 1989, "Studies of Mixed Convection in Vertical Tubes," *Int. J. Heat Fluid Flow*, Vol. 10, pp. 2-15.

Jacobitz, F. G., Sarkar, S., and Van ATTA, C. W., 1997, "Direct Numerical Simulations of the Turbulence Evolution in a Uniformly Sheared and Stably Stratified Flow," *J. Fluid Mech.*, Vol. 342, pp. 231-261.

Jacobson, S. A., and Reynolds, W. C., 1993, "Active Control of Boundary Layer Wall Shear Stress Using Self-Learning Neural Networks," *AIAA Paper 93-3272*.

Jimenez, J., and Moin, P., 1991, "The Minimal Flow Unit in Near-Wall Turbulence," *J. Fluid Mech.*, Vol. 225, pp. 213-240.

Jung, W. J., Mangiavacchi, N., and Akhavan, R., 1992, "Suppression of Turbulence in Wall-Bounded Flows by High-Frequency Spanwise Oscillations," *Phys. Fluids*, Vol. A4, pp. 1605-1607.

Karniadakis, G. E., and Henderson, R. D., 1998, "Spectral Element Methods for Incompressible Flows," *The Handbook of Fluid Dynamics*, R. W. Johnson, ed., CRC Press, pp. 29.1-41.

Kasagi, N., 1998, "Progress in Direct Numerical Simulation of Turbulent Transport and Its Control," *Int. J. Heat Fluid Flow*, Vol. 19, pp. 125-134.

Kasagi, N., and Hirata, M., 1977, "Bursting Phenomena in Turbulent Boundary Layer on a Horizontal Flat Plate Heated From Below," *Heat Transfer and Turbulent Buoyant convection*, D. B. Spalding and N. Afgan, eds., Hemisphere, Washington, D. C., Vol. 1, pp. 27-38.

Kasagi, N., and Nishimura, M., 1997, "Direct Numerical Simulation of Combined Forced and Natural Turbulent Convection in a Vertical Plane Channel," *Int. J. Heat Fluid Flow*, Vol. 18, pp. 88-99.

Kasagi, N., and Ohtsubo, Y., 1993, "Direct Numerical Simulation of Low Prandtl Number Thermal Fluid in a Turbulent Channel Flow," *Turbulent Shear Flows 8*, F. Durst et al., eds., Springer, Berlin, pp. 97-119.

Kasagi, N., and Shikazono, N., 1995, "Contribution of Direct Numerical Simulation to Understanding and Modeling Turbulent Transport," *Proc. R. Soc. Lond. A.*, Vol. 45, pp. 257-292.

Kasagi, N., Sumitani, Y., Suzuki, Y., and Iida, O., 1995, "Kinematics of the Quasi-Coherent Vortical Structure in Near-Wall Turbulence," *Int. J. Heat Fluid Flow*, Vol. 16, pp. 2-10.

Kasagi, N., Tomita, Y., and Kuroda, A., 1992, "Direct Numerical Simulation of the Passive Scalar Field in a Turbulent

Channel Flow," *ASME J. Heat Transfer*, Vol. 114, pp. 598-606.

Kawamura, H., Abe, H., Matsuo, Y., and Yamamoto, K., 1998, "DNS of Turbulent Heat Transfer in Channel Flow with respect to Reynolds-Number Effect," *2nd EF Conf. Turbulent Heat Transfer*, Manchester, Vol. 1, pp. 1.15-1.22.

Kawamura, H., Ohsaka, K., and Yamamoto, K., 1997, "DNS of Turbulent Heat transfer in Channel Flow with Low to Medium-High Prandtl Number Fluid," *Proc. 11th Symp. Turbulent Shear Flows*, Grenoble, Vol. 1, pp. 8.7-8.12.

Kays, W. M., and Crawford, M. E., 1980, "Convective Heat and Mass Transfer," 2nd ed., McGraw-Hill, NY.

Kim, J., 1990, personal communication.

Kim, J., and Moin, P., 1985, "Application of a Fractional-Step Method to Incompressible Navier-Stokes Equations," *J. Comput. Phys.*, Vol. 59, pp. 308-323.

Kim, J., and Moin, P., 1989, "Transport of Passive Scalars in a Turbulent Channel Flow," *Turbulent Shear Flows 6*, J.-C. Andre et al., eds., Springer, Berlin, pp. 85-96.

Kim, J., Moin, P., and Moser, R. D., 1987, "Turbulence Statistics in Fully Developed Channel Flow at Low Reynolds Number," *J. Fluid Mech.*, Vol. 177, pp. 133-166.

Komori, S., Ueda, H., Ogino, F., and Mizushima, T., 1983, "Turbulence Structure in Stably Stratified Open-Channel Flow," *J. Fluid Mech.*, Vol. 130, pp. 13-26.

Kreplin, H. P., and Eckelmann, H., 1979, "Behavior of the Three Fluctuating Velocity Components in the Wall Region of a Turbulent Channel Flow," *Phys. Fluids*, Vol. 22, pp. 1233-1239.

Kuroda, A., Kasagi, N., and Hirata, M., "A Direct Numerical Simulation of the Fully Developed Turbulent Channel Flow at a Very Low Reynolds Number," *Int. Symp. Computational Fluid Dynamics*, Nagoya, 1989, pp. 1174-1179; also in *Numerical Methods in Fluid Dynamics*, M. Yasuhara et al., eds, Vol. 2, J. Soc. Comp. Fluid Dyn., 1990, pp. 1012-1017.

Kuroda, A., Kasagi, N., and Hirata, M., 1995. "Direct Numerical Simulation of Turbulent Plane Couette-Poiseuille Flow: Effects of Mean Shear Rate on the Near-Wall Turbulence Structures," *Turbulent Shear Flows 9*, F. Durst et al., eds., Springer, Berlin, pp. 241-257.

Lauder, B. E., 1978, "Heat and Mass Transport," *Turbulence*, Topics in Applied Physics, P. Bradshaw, ed., Springer, Berlin, 231-287.

Le, H. L., and Moin, P., 1991, "An Improvement of Fractional Step Methods for the Incompressible Navier-Stokes Equations," *J. Comput. Phys.*, Vol. 92, pp. 369-379.

Lee, C., Kim, J., Babcock, D., and Goodman, R., 1997, "Application of Neural Network to Turbulence Control for Drag Reduction," *Phys. Fluids*, Vol. 9, pp. 1740-1747.

Lele, S. K., 1992, "Compact Finite Difference Schemes with Spectral-Like Resolution," *J. Comput. Phys.*, Vol. 103, pp.

16-42.

Lombardi, P., Angelis, V. D., and Banerjee, S., 1996, "Direct Numerical Simulation of Near-Interface Turbulence in Coupled Gas-Liquid Flow," *Phys. Fluids*, Vol. 8, pp. 1643-1665.

Lyons, S. L., and Hanratty, T. J., 1991, "Direct Numerical Simulation of Passive Heat Transfer in a Turbulent Channel Flow," *Int. J. Heat Mass Transfer*, Vol. 34, pp. 1149-1161.

Madabhushi, R. K., Balachandar, S., and Vanka, S. P., 1993, "A Divergence-Free Chebyshev Collocation Procedure for Incompressible Flows with Two Non-Periodic Directions," *J. Comput. Phys.*, Vol. 105, pp. 199-206.

McLaughlin, J. B., 1994, "Numerical Computation of Particle-Turbulence Interaction," *Int. J. Multiphase Flow*, Vol. 20, pp. s211-s232.

Mito, Y., and Kasagi, N., 1998, "DNS Study of Turbulence Modification with Streamwise-Uniform Sinusoidal Wall-Oscillation," *Int. J. Heat Fluid Flow*, Vol. 19, pp. 470-481.

Moin, P., and Bewley, T., 1994, "Feedback Control of Turbulence," *Appl. Mech. Rev.*, Vol. 47, pp. S3-S13.

Moin, P., and Bewley, T., 1995, "Application of Control Theory to Turbulence," *Proc. 12th Australian Fluid Mech. Conf.*, Sydney, pp. 10-15.

Moin, P., and Mahesh, K., 1998, "Direct Numerical Simulation: A Tool in Turbulence Research," *Ann. Rev. Fluid Mech.*, Vol. 30, pp. 539-578.

Moin, P., and Spalart, P. R., 1989, "Contributions of Numerical Simulation Data Bases to the Physics, Modelling, and Measurement of Turbulence," *Advances in Turbulence*, W. K. George and R. Arndt, eds., Hemisphere Publishing Corp., Washington, D. C., pp. 11-38.

Na, Y., Papavassiliou, D. V., and Hanratty, T. J., 1998, "Use of Direct Numerical Simulation to Study the Effect of Prandtl Number on Temperature Fields," *2nd EF Conf. Turbulent Heat Transfer, Manchester*, Vol. 1, pp. 1.3-1.14.

Nakajima, M., Fukui, K., Ueda, H., and Mizushima, T., 1980, "Buoyancy Effects on Turbulent Transport in Combined Free And Forced Convection Between Vertical Parallel Plates," *Int. J. Heat Mass Transfer*, Vol. 23, pp. 1325-1336.

Narashimha, R., and Sreenivasan, K. R., 1979, "Relaminarization of Fluid Flows," *Adv. Appl. Mech.*, Vol. 19, pp. 221-309.

Nishimura, M., and Kasagi, N., 1966, "Direct Numerical Simulation of Combined Forced and Natural Turbulent Convection in a Rotating Plane Channel," *Proc. 3rd KSME-JSME Therm. Eng. Conf.*, Kyongju, 1996, Vol. 3, pp. 77-82.

Nishino, N., and Kasagi, N., 1989, "Turbulence Statistics Measurement in a Two-Dimensional Channel Flow Using a Three-Dimensional Particle Tracking Velocimeter," *7th Symp. Turbulent Shear Flows*, Stanford, Vol. 2, pp. 22.1.1-22.1.6.

- Orlandi, P., and Fatica, M. 1997, "Direct Simulations of Turbulent Flow in a Pipe Rotating About its Axis," *J. Fluid Mech.*, Vol. 343, pp. 43-72.
- Orszag, S. A., 1980, "Spectral Methods for Problems in Complex Geometries," *J. Comput. Phys.*, Vol. 37, pp. 70-92.
- Pan, Y., and Banerjee, S., 1996, "Numerical Simulation of Particle Interactions with Wall Turbulence," *Phys. Fluids*, Vol. 8, pp. 2733-2755.
- Papavassiliou, D. V., and Hanratty, T. J., 1997, "Transport of a Passive Scalar in a Turbulent Channel Flow," *Int. J. Heat Mass Transfer*, Vol. 40, pp. 1303-1311.
- Patel, V. C., and Head, M. R., 1969, "Some Observations on Skin Friction and Velocity Profiles in Fully Developed Pipe and Channel Flows," *J. Fluid Mech.*, Vol. 38, pp. 181-201.
- Patera, A. T., 1984, "A Spectral Element Method for Fluid Dynamics: Laminar Flow in a Channel Expansion," *J. Comp. Physics*, Vol. 54, pp. 468-488.
- Pedinotti, S., Mariotti, G., and Banerjee, S., 1992, "Direct Numerical Simulation of Particle Behaviour in the Wall Region of Turbulent Flows in Horizontal Channels," *Int. J. Multiphase Flow*, Vol. 18, pp. 927-941.
- Peyret, R., and Taylor, T. D., 1983, "Computational Methods for Fluid Flow," Springer, Berlin.
- Rai, M. M., and Moin, P. 1991, "Direct Simulations of Turbulent Flow Using Finite-Difference Schemes," *J. Comput. Phys.*, Vol. 96, pp. 15-53.
- Rai, M. M., and Moin, P., 1993, "Direct Numerical Simulation of Transition and Turbulence in a Spatially Evolving Boundary Layer," *J. Comput. Phys.*, Vol. 109, pp. 169-192.
- Ranz, W. E., 1952, "Friction and Transfer Coefficient for Single Particle and Packed Beds," *Chemical Engineering Progress*, Vol. 48, pp. 247-253.
- Reynolds, W. C., 1990, "The Potential and Limitations of Direct and Large Eddy Simulations," *Whither Turbulence? - Turbulence at the Crossroads*, J. L. Lumley, ed., Springer, Berlin, pp. 313-342.
- Robinson, S. K., 1991, "The Kinematics of Turbulent Boundary Layer Structure," NASA TM-103859.
- Rogallo, R. S., and Moin, P., 1984, "Numerical Simulation of Turbulent Flows," *Ann. Rev. Fluid Mech.*, Vol. 16, pp. 99-137.
- Spalart, P. R., and Leonard, A., 1987, "Direct Numerical Simulation of Equilibrium Turbulent Boundary Layers," *Turbulent Shear Flows 5*, F. Durst et al., eds., Springer, Berlin, pp. 234-252.
- Spalart, P. R., Moser, R. D., and Rogers, M. M., 1991, "Spectral Methods for the Navier-Stokes Equations with One Infinite and Two Periodic Directions," *J. Comput. Phys.*, Vol. 96, pp. 297-324.
- Satake, S., and Kasagi, N., 1996, "Turbulence Control with Wall-Adjacent Thin Layer Damping Spanwise Velocity Fluctuations," *Int. J. Heat Fluid Flow*, Vol. 17, pp. 343-352.
- Satake, S., and Kasagi, N., 1997, "Suboptimal Turbulence Control with the Body Force of Selective Velocity Damping Localized to the Near-Wall Region," *Proc. 11th Symp. Turbulent Shear Flows*, Grenoble, Vol. 1, pp. P1-43-P1-48.
- Stull, R. B., 1988, "An Introduction to Boundary Layer Meteorology," Kluwer, Amsterdam.
- Sumitani, Y., and Kasagi, N., 1995, "Direct Numerical Simulation of Turbulent Transport with Uniform Wall Injection and Suction," *AIAA J.*, Vol. 33, pp. 1220-1228.
- Sussman, M., Smereka, P., and Osher, S., 1994, "A Level Set Approach for Computing Solution to Incompressible Two-Phase Flow," *J. Comput. Phys.*, Vol. 114, pp. 146-159.
- Suzuki, Y., and Kasagi, N., 1992, "Evaluation of Hot-Wire Measurements in Wall Shear Turbulence Using a Direct Numerical Simulation Database," *Exp. Therm. Fluid Sci.*, Vol. 5, pp. 69-77.
- Tennekes, H., and Lumley, J. L., 1972, "A First Course in Turbulence," MIT Press, Cambridge.
- Temam, R., 1984, "Navier-Stokes Equations," 3rd ed., North-Holland, Amsterdam.
- Tritton, D. J., 1988, "Physical Fluid Dynamics," 2nd ed., Oxford University Press, NY.
- Turner, J. S., 1973, "Buoyancy Effects in Fluids," Cambridge University Press, Cambridge.
- Yabe, T., and Aoki, T. "A Universal Solver for Hyperbolic Equations by Cubic-Polynomial Interpolation I, One-dimensional Solver," *Comp. Physics Comm.*, Vol. 66, pp. 219-232.
- Yamamoto, Y., Tanaka, T., and Tsuji, Y., 1998, "LES of Gas-Particle Turbulent Channel Flow (The Effect of Inter-Particle Collision on Structure of Particle Distribution)," *Proc. 3rd Int. Conf. Multiphase Flow*, Lyon, June 1998, in CD-Rom, P518.pdf, pp. 1-7.
- Yampolsky, J., 1979, "Spirally Fluted Tubing for Augmented Heat Transfer," General Atomic Company Report GA-A15442.
- Yano, T., and Kasagi, N., 1997, "Direct Numerical Simulation of Turbulent Heat Transport at High Prandtl Numbers," *Trans. JSEM*, Vol. 63, pp. 2840-2847, also *JSME Int. J.*, in press.
- Zang, Y., Street, R. L., and Koseff, J. R., 1994, "A Non-Staggered Grid, Fractional Step Method for Time-Dependent Incompressible Navier-Stokes Equations in Curvilinear Coordinates," *J. Comput. Phys.*, Vol. 114, pp. 18-33.